Properties of D and D^* mesons in the nuclear medium

L. Tolós,[1,*] C. García-Recio,[2] and J. Nieves[3]

[1]*Theory Group, KVI, University of Groningen, Zernikelaan 25, NL-9747 AA Groningen, The Netherlands*

[2]*Departamento de Física Atómica, Molecular y Nuclear, Universidad de Granada, E-18071 Granada, Spain*

[3]*Instituto de Física Corpuscular (Centro Mixto CSIC-UV), Institutos de Investigación de Paterna, Apartado 22085, E-46071 Valencia, Spain*

(Received 29 May 2009; revised manuscript received 9 November 2009; published 4 December 2009)

We study the properties of D and D^* mesons in nuclear matter within a simultaneous self-consistent coupled-channel unitary approach that implements heavy-quark symmetry. The in-medium solution accounts for Pauli blocking effects and for the D and D^* self-energies in a self-consistent manner. We pay special attention to renormalization of the intermediate propagators in the medium beyond the usual cutoff scheme. We analyze the behavior in the nuclear medium of the rich spectrum of dynamically generated baryonic resonances in the $C = 1$ and $S = 0$ sector and their influence on the self-energy and, hence, the spectral function of D and D^* mesons. The D meson quasiparticle peak mixes with $\Sigma_c(2823)N^{-1}$ and $\Sigma_c(2868)N^{-1}$ states, whereas the $\Lambda_c(2595)N^{-1}$ mode is present in the low-energy tail of the spectral function. The D^* spectral function incorporates $J = 3/2$ resonances, and $\Sigma_c(2902)N^{-1}$ and $\Lambda_c(2941)N^{-1}$ fully determine the behavior of D^* meson spectral function at the quasiparticle peak. As the density increases, these resonant-hole modes tend to smear out and the spectral functions become broad. We also obtain the D and D^* scattering lengths and the optical potentials for different density regimes. The D meson potential stays attractive, whereas the D^* meson one is repulsive with increasing densities up to twice that of the normal nuclear matter. Compared to previous in-medium SU(4) models, we obtain similar values for the real part of the D meson potential but much smaller imaginary parts. This result could have important implications for the observation of D^0-nucleus bound states.

DOI: 10.1103/PhysRevC.80.065202 PACS number(s): 11.10.St, 14.20.Lq, 14.40.Lb, 21.65.−f

I. INTRODUCTION

Interest in the properties of open and hidden charmed mesons was triggered more than 20 years ago in the context of relativistic nucleus-nucleus collisions in connection with charmonium suppression [1] as a probe for the formation of quark-gluon plasma (QGP). The experimental program in hadronic physics at the future FAIR facility at GSI [2] will move from the light quark sector to the heavy one and will face new challenges where charm plays a dominant role. In particular, a large part of the PANDA physics program will be devoted to charmonium spectroscopy. Moreover, the CBM experiment will extend the GSI program for in-medium modification of hadrons in the light quark sector and provide the first insight into the charm-nucleus interaction.

The primary theoretical effort is to understand the interaction between hadrons and the charm degree of freedom. Charmed baryonic resonances have recently received a lot of attention, motivated by the discovery of quite a few new states by the CLEO, Belle, and BABAR Collaborations [3–8]. Whether those resonances have the usual qqq structure or qualify better as being dynamically generated via meson-baryon scattering processes is a matter of great interest. In fact, the unitarization, in coupled channels, of the chiral perturbation amplitudes for scattering of 0^- octet Goldstone bosons off baryons of the nucleon $1/2^+$ octet has proven to be quite successful in the charmless sector [9–28]. The modification of the various meson-baryon amplitudes for the case of finite temperature and/or nuclear density has also attracted a lot of attention and has been discussed in detail [29–34].

Extension of the unitarized meson-baryon method to the charm sector was attempted in a first exploratory work in Ref. [35], where the free-space amplitudes were constructed from a set of separable coupled-channel interactions obtained from chirally motivated Lagrangians upon replacing the s quark with the c quark. A different approach resulting from the scattering of Goldstone bosons off the ground-state $1/2^+$ charmed baryons was pursued in Ref. [18], but the most substantial improvement in constructing the meson-baryon interaction in the charm sector came from exploiting the universal vector-meson coupling hypothesis to break the SU(4) symmetry [36]. The t-channel exchange of vector mesons (TVME) between pseudoscalar mesons and baryons preserved chiral symmetry in the light meson sector keeping the Weinberg-Tomozawa (WT) type of interaction. An extension to d-wave $J = 3/2^-$ resonances was developed in Ref. [37], whereas some modifications of the model in Ref. [36] were implemented in Ref. [38], both in the kernel and in the renormalization scheme. More recently, there have been attempts to construct the DN and $\bar{D}N$ interaction by incorporating the charm degree of freedom in the SU(3) meson exchange model of the Jülich group [39,40].

Nuclear medium modifications were then incorporated to study the properties of charmed mesons in nuclear matter and the influence of those modifications in the charmonium production rhythm at finite baryon densities. Possible variation of this rhythm might indicate the formation of the QGP phase of QCD at high densities. Previous works based on mean-field approaches provided important mass shifts for the D and $\bar{D}$ meson masses [41–44]. Some of those models have

*tolos@kvi.nl

recently been revised [45,46]. However, the spectral features of D mesons in symmetric nuclear matter were obtained for the first time in the exploratory work in Ref. [35], whereas finite temperature effects were incorporated later, in Ref. [47]. Afterward, within the SU(4) TVME model in Ref. [36], the properties of $(D,\bar{D})$ and $(D_s,\ \bar{D}_s)$ mesons were analyzed in Refs. [38,48,49]. In the latter reference, the kernel and renormalization scheme employed in Ref. [36] were modified.

However, these SU(4) TVME-inspired models are not consistent with heavy-quark symmetry (HQS), which is a proper QCD spin-flavor symmetry that appears when the quark masses, such as the charm mass, become larger than the typical confinement scale. As a consequence of this symmetry, spin interactions vanish for infinitely massive quarks. Thus, heavy hadrons come in doublets (if the spin of the light degrees of freedom is not zero), which are degenerated in the infinite quark-mass limit. And this is the case for the D meson and its vector partner, the D^* meson.

In fact, the incorporation of vector mesons into the coupled-channel picture has been pursued very recently in the strange sector. On one hand, vector mesons have been incorporated within the hidden-gauge formalism. Within this scheme, a broad spectrum of new resonant meson-baryon states has been generated [50–52]. On the other hand, the WT meson-baryon chiral Lagrangian has also been extended to account for vector meson degrees of freedom by means of a scheme that starts from a SU(6) spin-flavor symmetry Lagrangian and that incorporates some symmetry-breaking corrections determined by physical masses and meson decay constants [53–56]. The corresponding Bethe-Salpeter equation reproduces the previous SU(3) flavor WT results for the lowest lying s and d waves and negative-parity baryon resonances and gives new information on more massive states, for example, the $\Lambda(1800)$ and $\Lambda(2325)$ resonances. Extension of this scheme to four flavors, incorporating the charm degree of freedom, was carried out in Ref. [57], and it automatically incorporates HQS in the charm sector, improving in this respect on the SU(4) TVME models, as D and D^* mesons are thus consistently treated. One of the distinctive differences of this approach with respect to those built in the SU(4) TVME model lies in the wave-function content of the resonances. Thus, for instance, the dynamics of the lowest lying resonance $\Lambda_c(2595)$ is completely dominated by the DN channel in the SU(4) TVME model in Ref. [36], whereas it turns out to be largely a D^*N state within the SU(8) scheme in Ref. [57]. Such differences might also have a direct influence on the dynamics at finite densities.

Thus, in this work, we aim to investigate the nuclear medium effects in hadronic systems with a charm of one ($C = 1$) and no strangeness ($S = 0$) within the SU(8) model derived in Ref. [57]. In particular, we study the dynamically generated baryonic resonances in free space, as well as in the nuclear medium, to analyze how the masses and widths are modified with density. We also study the D and D^* meson self-energies in the nuclear medium, calculating their spectral functions for a variety of densities and the corresponding optical potentials. A novelty of our work is that we simultaneously obtain, in a self-consistent manner, the D and D^* meson self-energies. We then compare our results with the previous ones obtained within SU(4) TVME schemes and other simpler models [35,38,47–49], also paying special attention to regularization of the intermediate propagators in the medium beyond the cutoff method. Nuclear medium effects for hadronic scattering amplitudes and for hadron propagators are of interest for the understanding and correct interpretation of data obtained in heavy-ion collisions where the high nuclear densities reached can substantially change the properties of the involved hadrons.

To end this introduction, and before we start deriving the D and D^* self-energies in a nuclear medium, we would like to make a general reflection to better situate this work. Although the model in Ref. [57] is possibly the best one existing in the literature for describing the free-space $C = 1$, $S = 0$, meson-baryon elastic scattering at low energies,[1] it does not provide, as is the case for the rest of the available models, the correct analytical properties of the scattering matrix, including s, t, and u cuts and proper crossing symmetry. Only the real theory, presumably QCD, could do that. However, one should bear in mind that deficiencies of the free-space model would definitely affect the results presented here for amplitudes embedded in cold nuclear matter. Because we aim to describe resonances, it is important to use a model consistent with the unitarity cut, such as that in Ref. [57], whereas one hopes for the rest of the analytical properties to be partially taken into account thanks to the low energy constants (subtraction constants, etc.). To ignore a cut that would cover totally or partially the studied resonance region is not so important;[2] what is more relevant is the proximity of a resonance to a branching point, where the amplitude might vary more rapidly, together with the strength of the coupling of the resonance to the given channel. The free-space model in Ref. [57] only properly accounts for the two-body unitarity cut, and it thus suffers from some limitations. For example, this model does not account for the dynamics of an intermediate nucleon in the u-channel diagram $DN \to \Lambda_c\rho$, involving two p-wave couplings ($DN\Lambda_c$ and $NN\rho$), which gives rise to a cut extending from 1.55 to 2.74 GeV. The lowest energy branch point should not suppose a serious problem. On the other hand, $\Lambda_c\rho$ selects isospin $I = 1$, and if one examines Tables VI and IX in Ref. [57], one sees no resonances excessively close to the branch point at 2.74 GeV, with a dominant coupling to that channel. Thus, although some effects will exist, we do not expect drastic changes that could lead us to think that the interaction model in Ref. [57] is unrealistic, especially close to threshold, where p-wave couplings will be negligible.

Other contributions not considered in the model in Ref. [57] are those driven by the exchange of a pion in the t channel. All of them that contribute to the $DN \to D^*N$ amplitude could

[1] As outlined earlier, it provides a scheme for four flavors and for pseudoscalar and vector mesons that reduces to the WT interaction in the sector where Goldstone bosons are involved and that incorporates HQS in the charm sector.

[2] For instance, the t-channel ρ-exchange cut for the elastic $\bar{D}^*\Sigma_c^*$ amplitude goes from about 0.53 to 4.45 GeV. Obviously, one does not need to consider this cut explicitly when studying elastic πN scattering in the region of the $\Delta(1232)$ resonance.

be quite relevant, as this might induce a pronounced energy dependence, which would be difficult to account for by means of the low energy constants of the model.[3] This contribution again involves two p-wave vertices, which would vanish at the D^*N threshold. Below the threshold, its contribution would depend strongly on the adopted form factors to account for the off-shellness. This t-pion exchange contribution can be safely neglected at threshold. Above threshold, and because the D and D^* meson masses are quite similar, the exchanged virtual pion will carry a low energy, and therefore in good approximation $q^2 \sim -\vec{q}^2$. Keeping in mind the existence of two p-wave vertices in the diagram, each of them proportional to the virtual pion momentum, we expect a large cancellation of these with the pion propagator (neglecting the pion mass), which will significantly reduce the energy dependence of this contribution.

From the preceding discussion, it is clear that the predictions of the model in Ref. [57] far from threshold are likely subject to large uncertainties due to the contributions mentioned previously (pion exchanges in the t channel and u-cut contributions) and possibly other mechanisms. This is why in this work we have only computed properties of the in-medium amplitudes close to threshold.

II. FORMALISM: THE DN AND D^*N INTERACTION IN NUCLEAR MATTER

We calculate the self-energy of D and D^* mesons in nuclear matter from a self-consistent calculation in coupled channels that treats the heavy pseudoscalar and vector mesons on equal footing, as required by HQS. To incorporate HQS into the meson-baryon interaction we extend the WT meson-baryon Lagrangian to the SU(8) spin-flavor symmetry group [57]. We start from the traditional three-flavor WT Lagrangian, which is not just SU(3) symmetric but also chiral $[\mathrm{SU}_L(3) \otimes \mathrm{SU}_R(3)]$ invariant. Symbolically, up to an overall constant, the WT interaction is

$$\mathcal{L}_{\mathrm{WT}} = \mathrm{Tr}([M^\dagger, M][B^\dagger, B]), \tag{1}$$

where mesons (M) and baryons (B) fall in SU(3) representation **8**, which is the adjoint representation. The commutator indicates a t-channel coupling to the $\mathbf{8}_a$ (antisymmetric) representation. For the SU(8) spin-flavor symmetry, mesons M fall in the **63** (adjoint) representation and baryons B are found in the **120** representation, which is fully symmetric. The group reductions,

$$\begin{aligned} \mathbf{63} \otimes \mathbf{63} &= \mathbf{1} \oplus \mathbf{63}_s \oplus \mathbf{63}_a \oplus \mathbf{720} \oplus \mathbf{945} \oplus \mathbf{945}^* \oplus \mathbf{1232}, \\ \mathbf{120} \otimes \mathbf{120}^* &= \mathbf{1} \oplus \mathbf{63} \oplus \mathbf{1232} \oplus \mathbf{13104}, \end{aligned} \tag{2}$$

lead to a total of four different t-channel SU(8) singlet couplings, which can be used to construct s-wave meson-baryon interactions:

$$\begin{aligned} &[(M^\dagger \otimes M)_{\mathbf{1}} \otimes (B^\dagger \otimes B)_{\mathbf{1}}]_{\mathbf{1}}, \\ &[(M^\dagger \otimes M)_{\mathbf{63}_a} \otimes (B^\dagger \otimes B)_{\mathbf{63}}]_{\mathbf{1}}, \\ &[(M^\dagger \otimes M)_{\mathbf{63}_s} \otimes (B^\dagger \otimes B)_{\mathbf{63}}]_{\mathbf{1}}, \\ &[(M^\dagger \otimes M)_{\mathbf{1232}} \otimes (B^\dagger \otimes B)_{\mathbf{1232}}]_{\mathbf{1}}. \end{aligned} \tag{3}$$

To ensure that the SU(8) amplitudes will reduce to those deduced from the SU(3) WT Lagrangian in the $(\mathbf{8_1})$ meson-$(\mathbf{8_2})$ baryon subspace [denoting the SU(3) multiplets of dimensionality $\mathbf{n}$ and spin J as $\mathbf{n_{2J+1}}$], we set all the couplings in Eq. (3) to be zero except for

$$\mathcal{L}_{\mathrm{WT}}^{\mathrm{SU(8)}} = [(M^\dagger \otimes M)_{\mathbf{63}_a} \otimes (B^\dagger \otimes B)_{\mathbf{63}}]_{\mathbf{1}}, \tag{4}$$

which is the natural and unique SU(8) extension of the usual SU(3) WT Lagrangian. To compute the matrix elements of the SU(8) WT interaction $\mathcal{L}_{\mathrm{WT}}^{\mathrm{SU(8)}}$, we use quark model constructions of hadrons with field theoretical methods to express everything in tensor representations as described in Appendix A in Ref. [57]. Thus, we get the tree-level amplitudes (using the convention $V = -\mathcal{L}$)

$$V_{ab}^{IJSC}(\sqrt{s}) = D_{ab}^{IJSC} \frac{\sqrt{s} - M}{2f^2} \left(\sqrt{\frac{E+M}{2M}} \right)^2, \tag{5}$$

where the last factor is due to the spinor normalization convention: $\bar{u}u = \bar{v}v = 1$, as in Refs. [20,22]. In expression (5) $IJSC$ are the meson-baryon isospin, total angular momentum, strangeness, and charm quantum numbers, respectively; $M(E)$ is the common mass (CM energy) of the baryons placed in the **120** SU(8) representation; and D^{IJSC} is a matrix in the coupled-channel space (see Ref. [57]).

However, the SU(8) spin flavor is strongly broken in nature. The breaking of SU(8) is twofold. On one hand, we take into account mass-breaking effects by adopting the physical hadron masses in the tree-level interactions in Eq. (5) and in evaluation of the kinematic thresholds of different channels. On the other hand, we consider the difference between the weak noncharmed and charmed pseudoscalar and vector meson decay constants. Then our tree-level amplitudes read

$$\begin{aligned} V_{ab}^{IJSC}(\sqrt{s}) = D_{ab}^{IJSC} &\frac{2\sqrt{s} - M_a - M_b}{4 f_a f_b} \\ &\times \sqrt{\frac{E_a + M_a}{2M_a}} \sqrt{\frac{E_b + M_b}{2M_b}}, \end{aligned} \tag{6}$$

where M_a (M_b) and E_a (E_b) are, respectively, the mass and the CM energy of the baryon in the a (b) channel. We focus on the nonstrange ($S = 0$) and singly charmed ($C = 1$) sector, where DN and D^*N are embedded. In particular, we look at $I = 0$ and $I = 1$ channels for $J = 1/2$ and $J = 3/2$. Channels involved in the coupled-channel calculation are listed in Table I, where below every channel we indicate its mass threshold, $M + m$, in MeV. Compared to Ref. [57], we take $M_\Delta = 1232$ MeV, instead of the pole mass. As a consequence, resonances that couple strongly to channels with a Δ component might change their position and width slightly, as in the case of ($I = 1$,

[3]Previous models [18,35,36,38] also ignored this contribution because in these works D^* degrees of freedom were not explicitly taken into account in the external legs. But, as we have commented, ignoring such degrees of freedom was totally unjustified.

TABLE I. A list of all involved baryon-meson channels for each isospin IJ sector, with their mass thresholds (in MeV), $M + m$, shown below their names.

$I = 0, J = 1/2$									
		$\Sigma_c\pi$	ND	$\Lambda_c\eta$	ND^*	Ξ_cK	$\Lambda_c\omega$	$\Xi_c'K$	ΛD_s
		2591.6	2806.15	2833.97	2947.54	2965.11	3069.11	3072.51	3084.18
		ΛD_s^*	$\Sigma_c\rho$	$\Lambda_c\eta'$	$\Sigma_c^*\rho$	$\Lambda_c\phi$	Ξ_cK^*	$\Xi_c'K^*$	$\Xi_c^*K^*$
		3227.98	3229.05	3244.24	3293.46	3305.92	3361.11	3468.51	3538.01
$I = 1, J = 1/2$									
$\Lambda_c\pi$	$\Sigma_c\pi$	ND	ND^*	Ξ_cK	$\Sigma_c\eta$	$\Lambda_c\rho$	$\Xi_c'K$	ΣD_s	$\Sigma_c\rho$	$\Sigma_c\omega$
2424.5	2591.6	2806.15	2947.54	2965.12	3001.07	3061.95	3072.52	3161.64	3229.05	3236.21
ΔD^*	$\Sigma_c^*\rho$	$\Sigma_c^*\omega$	ΣD_s^*	Ξ_cK^*	$\Sigma_c\eta'$	$\Xi_c'K^*$	$\Sigma_c\phi$	$\Sigma^*D_s^*$	$\Sigma_c^*\phi$	$\Xi_c^*K^*$
3240.62	3293.46	3300.62	3305.45	3361.11	3411.34	3468.51	3473.01	3496.87	3537.42	3538.01
$I = 0, J = 3/2$									
$\Sigma_c^*\pi$	ND^*	$\Lambda_c\omega$	Ξ_c^*K	ΛD_s^*	$\Sigma_c\rho$	$\Sigma_c^*\rho$	$\Lambda_c\phi$	Ξ_cK^*	$\Xi_c'K^*$	$\Xi_c^*K^*$
2656.01	2947.54	3069.11	3142.01	3227.98	3229.05	3293.46	3305.92	3361.11	3468.51	3538.01
$I = 1, J = 3/2$									
	$\Sigma_c^*\pi$	ND^*	$\Lambda_c\rho$	$\Sigma_c^*\eta$	ΔD	Ξ_c^*K	$\Sigma_c\rho$	$\Sigma_c\omega$	ΔD^*	$\Sigma_c^*\rho$
	2656.01	2947.54	3061.95	3065.48	3099.23	3142.02	3229.05	3236.21	3240.62	3293.46
	$\Sigma_c^*\omega$	ΣD_s^*	Σ^*D_s	Ξ_cK^*	$\Xi_c'K^*$	$\Sigma_c\phi$	$\Sigma_c^*\eta'$	$\Sigma^*D_s^*$	$\Sigma_c^*\phi$	$\Xi_c^*K^*$
	3300.62	3305.45	3353.06	3361.11	3468.51	3473.01	3475.75	3496.87	3537.42	3538.01

$J = 1/2$) $\Sigma_c(2556)$ and ($I = 1$, $J = 3/2$) $\Sigma_c(2554)$, to a few MeV above the values in Ref. [57]. We also take $m_{K^*} = 892$ MeV. In addition, we use experimental, when possible, or theoretical estimates for the meson decay constants. The values used in this work are given in Table II in Ref. [57].

With the kernel of the meson-baryon interaction given in Eq. (6), we obtain the coupled DN and D^*N effective interaction in free space by solving the on-shell Bethe-Salpeter equation [11,14,15,22,58,59],

$$T^{IJ}(\sqrt{s}) = \frac{1}{1 - V^{IJ}(\sqrt{s})G^{0(IJ)}(\sqrt{s})} V^{IJ}(\sqrt{s}), \tag{7}$$

in the coupled-channel space. Here $G^{0(IJ)}(\sqrt{s})$ is a diagonal matrix consisting of loop functions. The free-space loop function for channel a reads

$$G_a^{0(IJ)}(\sqrt{s}) = \mathrm{i}2M_a \int \frac{d^4q}{(2\pi)^4} D^0_{\mathcal{B}_a}(P-q) D^0_{\mathcal{M}_a}(q), \tag{8}$$

$$D^0_{\mathcal{B}_a}(P-q) = \left[(P-q)^2 - M_a^2 + i\varepsilon\right]^{-1}, \tag{9}$$

$$D^0_{\mathcal{M}_a}(q) = \left(q^2 - m_a^2 + i\varepsilon\right)^{-1}, \tag{10}$$

where $s = P^2$, D^0 is a free hadron propagator, a runs in the allowed baryon-meson channels for the given IJ sector, and M_a and m_a are the masses of baryon $\mathcal{B}_a$ and meson $\mathcal{M}_a$ in channel a, respectively. The previously defined loop function is ultraviolet (UV) divergent. However, the difference $G^0(\sqrt{s_1}) - G^0(\sqrt{s_2})$ is finite for any finite values of s_1 and s_2; hence, the function can be regularized by setting a finite value of G^0 at a given point. We choose

$$G_a^{0(IJ)}\left(\sqrt{s} = \mu_a^{IJ}\right) = 0, \tag{11}$$

with index a running in the coupled-channel space, as done in Refs. [36,37,57]. In those works, the subtraction point was taken to be independent of a and J as

$$(\mu^I)^2 = \alpha\left(m_{\mathrm{th}}^2 + M_{\mathrm{th}}^2\right), \tag{12}$$

where m_{th} and M_{th} are the meson and baryon masses of the hadronic channel with the lowest mass threshold for a fixed I and arbitrary J. The value of $\alpha = 0.9698$ was adjusted to reproduce the position of the well-established $\Lambda_c(2595)$ resonance with $IJ = (0, 1/2)$. Then the same value was used in all other sectors. In this work we follow the same prescription, taking $(\mu^{I=0})^2 = \alpha({M_{\Sigma_c}}^2 + m_\pi^2)$ and $(\mu^{I=1})^2 = \alpha({M_{\Lambda_c}}^2 + m_\pi^2)$.

Hence, the renormalized (finite) loop function finally reads

$$G^0(\sqrt{s}) = \mathrm{i}2M \int \frac{d^4q}{(2\pi)^4} \left[D^0_{\mathcal{B}}(P-q) D^0_{\mathcal{M}}(q) - D^0_{\mathcal{B}}(\bar{P}-q) D^0_{\mathcal{M}}(q)\right], \tag{13}$$

with P and $\bar{P}$ defined such that $P^2 = s$ and $\bar{P}^2 = (\mu^I)^2$, where, for simplicity, the obvious isospin I, spin J, and channel a labels have been omitted. This is the (standard) method we use to renormalize the free baryon-meson loop.

The properties of D and D^* mesons in nuclear matter are obtained by incorporating the corresponding medium modifications in the effective DN and D^*N interactions. One of the sources of density dependence comes from the Pauli principle acting on the nucleons. Another source is related to the change in the properties of mesons and baryons in the intermediate states due to the interaction with nucleons of the Fermi sea.

These changes are implemented by using the in-medium hadron propagators instead of the corresponding free ones. Therefore, we should define a consistent renormalization scheme, similar to that adopted in the free case, for the loop function in a nuclear medium with density ρ.

Let us first review what has been done before. The in-medium loop function G^ρ_Λ, used in Refs. [38,49], depends on a regularization cutoff Λ that renders the UV divergence finite, and it is defined as

$$G^\rho_\Lambda(P) = \mathrm{i}2M \int_\Lambda \frac{d^4q}{(2\pi)^4} D^\rho_{\mathcal{B}}(P-q) D^\rho_{\mathcal{M}}(q), \qquad (14)$$

where $D^\rho_{\mathcal{B}}$ and $D^\rho_{\mathcal{M}}$ are the hadron propagators in a medium with density ρ. In those works [38,49], the three-momentum cutoff Λ is fixed in such a way that the free ($\rho = 0$) results reproduce certain known experimental results [e.g., the position of the resonance $\Lambda_c(2595)$ for the sector with quantum numbers $IJSC = 0, 1/2, 0, 1$]. This way of regularizing the UV loop function induces medium corrections of the type

$$\begin{aligned} G^\rho_\Lambda(P) &= G^0_\Lambda(\sqrt{s}) + \delta G^\rho_\Lambda(P), \\ \delta G^\rho_\Lambda(P) &\equiv G^\rho_\Lambda(P) - G^0_\Lambda(\sqrt{s}) = \mathrm{i}2M \int_\Lambda \frac{d^4q}{(2\pi)^4} \\ &\quad \times \left[D^\rho_{\mathcal{B}}(P-q) D^\rho_{\mathcal{M}}(q) - D^0_{\mathcal{B}}(P-q) D^0_{\mathcal{M}}(q) \right]. \end{aligned} \qquad (15)$$

In this work, we do want to avoid finite-cutoff effects. So we define the in-medium loop function as the free one G^0, given in Eq. (13) and defined as in Refs. [36,37,53,55–57] without having to introduce any cutoff, plus a term that accounts for the same kind of medium effects as displayed in Eq. (15), but taking Λ large enough (i.e., $\Lambda \to \infty$). Hence, we use

$$\begin{aligned} G^\rho(P) &= G^0(\sqrt{s}) + \delta G^\rho(P), \\ \delta G^\rho(P) &= \lim_{\Lambda\to\infty} \delta G^\rho_\Lambda(P) \equiv \mathrm{i}2M \int \frac{d^4q}{(2\pi)^4} \left[D^\rho_{\mathcal{B}}(P-q) D^\rho_{\mathcal{M}}(q) \right. \\ &\quad \left. - D^0_{\mathcal{B}}(P-q) D^0_{\mathcal{M}}(q) \right]. \end{aligned} \qquad (16)$$

The UV finite δG^ρ correction contains all the nuclear medium effects affecting the loop, and it is independent of the selected subtracting point used to regularize it. Thus a cutoff is not needed for the calculation. The defined loop function at finite density G^ρ can be rewritten as

$$\begin{aligned} G^\rho(P) = \mathrm{i}2M \int \frac{d^4q}{(2\pi)^4} &\left[D^\rho_{\mathcal{B}}(P-q) D^\rho_{\mathcal{M}}(q) \right. \\ &\left. - D^0_{\mathcal{B}}(\bar{P}-q) D^0_{\mathcal{M}}(q) \right], \end{aligned} \qquad (17)$$

where the integrand is the difference between two terms. The first one corresponds to the baryon and meson propagators calculated at density ρ and total momentum P. The second term depends neither on the density nor on P, and it is constructed from propagators evaluated at $\rho = 0$ and with fixed total momentum $\bar{P}$, such that $\bar{P}^2 = (\mu^I)^2$. This shows that our prescription of Eq. (16) for G^ρ amounts to assuming that the subtraction employed to make the UV divergent function finite is independent of the nuclear density.

For practical numerical purposes we calculate G^ρ as specified in Eq. (16), where the free part is analytical, regularized with a subtracting constant, and well known, and the medium modification part δG^ρ is numerically evaluated in the same way as for G^ρ_Λ in previous work but taking into account that it has a subtracted part G^0, providing a δG^ρ that is UV finite.

For the DN and D^*N channels, we consider Pauli blocking effects on the nucleons together with self-energy insertions of the D and D^* mesons. The self-energy is obtained self-consistently from the in-medium DN and D^*N effective interactions $T^\rho{}_{D(D^*)N}$, as we show in the following. The corresponding in-medium single-particle propagators are given by

$$\begin{aligned} D^\rho_N(p) &= \frac{1}{2E_N(\vec{p})} \left[\frac{1-n(\vec{p})}{p^0 - E_N(\vec{p}) + i\varepsilon} + \frac{n(\vec{p})}{p^0 - E_N(\vec{p}) - i\varepsilon} \right. \\ &\quad \left. + \frac{1}{-p^0 - E_N(\vec{p}) + i\varepsilon} \right] \\ &= D^0_N(p) + 2\pi i n(\vec{p}) \frac{\delta\left[p^0 - E_N(\vec{p})\right]}{2E_N(\vec{p})}, \end{aligned} \qquad (18)$$

$$\begin{aligned} D^\rho_{D(D^*)}(q) &= \left[(q^0)^2 - \omega(\vec{q})^2 - \Pi_{D(D^*)}(q) \right]^{-1} \\ &= \int_0^\infty d\omega \left[\frac{S_{D(D^*)}(\omega, \vec{q})}{q^0 - \omega + i\varepsilon} - \frac{S_{\bar{D}(\bar{D}^*)}(\omega, \vec{q})}{q^0 + \omega - i\varepsilon} \right], \end{aligned} \qquad (19)$$

where $E_N(\vec{p}) = \sqrt{\vec{p}^2 + M_N^2}$, $\omega(\vec{q}) = \sqrt{\vec{q}^2 + m^2_{D(D^*)}}$, $\Pi_{D(D^*)}(q^0, \vec{q})$ is the $D(D^*)$ meson self-energy, and $S_{D(D^*)}$ is the corresponding meson spectral function. In a very good approximation the spectral function for $\bar{D}$ can be approximated by the free-space one, that is, by a delta function, because for the case $C = -1$, there are no low-lying baryon resonances. Finally, $n(\vec{p})$ is the Fermi gas nucleon momentum distribution, given by the step function $n(\vec{p}) = H(k_F - |\vec{p}|)$, with $k_F = (3\pi^2\rho/2)^{1/3}$.

Using Eq. (16) and performing the energy integral over q^0, the DN and D^*N loop functions read

$$\begin{aligned} G^\rho{}_{D(D^*)N}(P) &= G^0_{D(D^*)N}(\sqrt{s}) + \int \frac{d^3q}{(2\pi)^3} \frac{M_N}{E_N(\vec{p})} \\ &\times \left\{ \frac{-n(\vec{p})}{[P^0 - E_N(\vec{p})]^2 - \omega(\vec{q})^2 + i\varepsilon} + [1 - n(\vec{p})] \left(\frac{-1/[2\omega(\vec{q})]}{P^0 - E_N(\vec{p}) - \omega(\vec{q}) + i\varepsilon} + \int_0^\infty d\omega \frac{S_{D(D^*)}(\omega, \vec{q})}{P^0 - E_N(\vec{p}) - \omega + i\varepsilon} \right) \right\} \Big|_{\vec{p} = \vec{P} - \vec{q}}, \end{aligned} \qquad (20)$$

where the first term of the integral, proportional to $-n(\vec{p})$, is what we call the Pauli correction and accounts for the case where the Pauli blocking on the nucleon is considered and the meson in-medium self-energy is neglected. The second term, proportional to $[1-n(\vec{p})]$, is exactly zero if the meson spectral function $S_{D(D^*)}$ is taken to be the free one, $S^{\rm free}_{D(D^*)}(\omega,\vec{q}) = \delta[\omega-\omega(\vec{q})]/(2\omega)$. Thus, it accounts for the contribution of the in-medium meson modification to the loop function. Note that, unlike in Refs. [38,49], we also include the antiparticle contributions in the propagators.

As for $D\Delta$ and $D^*\Delta$ channels, we include the self-energy of the D and D^* mesons. Then the equivalent of Eq. (20) for those channels reads

$$G^{\rho}{}_{D(D^*)\Delta}(P) = G^0_{D(D^*)\Delta}(\sqrt{s}) + \int \frac{d^3q}{(2\pi)^3}\frac{M_\Delta}{E_\Delta(\vec{p})} \times \left\{ \frac{-1/[2\omega(\vec{q})]}{P^0 - E_\Delta(\vec{p}) - \omega(\vec{q}) + i\varepsilon} + \int_0^\infty d\omega \frac{S_{D(D^*)}(\omega,\vec{q})}{P^0 - E_\Delta(\vec{p}) - \omega + i\varepsilon} \right\}\Big|_{\vec{p}=\vec{P}-\vec{q}}. \quad (21)$$

For other channels that couple to DN and D^*N (see Table I), we refrain from including any medium modifications in the loop function, and therefore, we use the free-space one given in Eq. (13). This is due to the lack of knowledge of how the properties of some mesons, such as ρ and ω, change in the medium. Only pions in nuclear matter have been intensively studied [60,61], but, as indicated in Ref. [57] and discussed in the next section, coupling to intermediate states with pions is of minor importance for the dynamic generation of baryon resonances in the $S=0$ and $C=1$ sector, which governs the DN and D^*N dynamics in nuclear matter.

We can now solve the on-shell Bethe-Salpeter equation in nuclear matter for the in-medium amplitudes,

$$T^{\rho(IJ)}(P) = \frac{1}{1 - V^{IJ}(\sqrt{s})G^{\rho(IJ)}(P)} V^{IJ}(\sqrt{s}). \quad (22)$$

The in-medium D and D^* self-energies are finally obtained by integrating $T^{\rho}{}_{D(D^*)N}$ over the nucleon Fermi sea,

$$\Pi_D(q^0,\vec{q}) = \int \frac{d^3p}{(2\pi)^3} n(\vec{p}) \left[T^{\rho\,(I=0,J=1/2)}_{DN}(P^0,\vec{P}) + 3T^{\rho\,(I=1,J=1/2)}_{DN}(P^0,\vec{P}) \right], \quad (23)$$

$$\Pi_{D^*}(q^0,\vec{q}) = \int \frac{d^3p}{(2\pi)^3} n(\vec{p}) \left[\frac{1}{3} T^{\rho\,(I=0,J=1/2)}_{D^*N}(P^0,\vec{P}) + T^{\rho\,(I=1,J=1/2)}_{D^*N}(P^0,\vec{P}) + \frac{2}{3} T^{\rho\,(I=0,J=3/2)}_{D^*N}(P^0,\vec{P}) + 2T^{\rho\,(I=1,J=3/2)}_{D^*N}(P^0,\vec{P}) \right], \quad (24)$$

where $P^0 = q^0 + E_N(\vec{p})$ and $\vec{P} = \vec{q} + \vec{p}$ are the total energy and momentum of the DN (D^*N) pair in the nuclear matter rest frame and the values $(q^0,\vec{q})$ are the energy and momentum of the D and D^* meson also in this frame. $\Pi_{D(D^*)}(q^0,\vec{q})$ has to be determined self-consistently, as it is obtained from the in-medium amplitude $T^{\rho}_{D(D^*)N}$, which contains the $D(D^*)N$ loop function $G^{\rho}_{D(D^*)N}$, and the latter quantity is itself a function of $\Pi_{D(D^*)}(q^0,\vec{q})$. From this we obtain the corresponding spectral function to complete the integral for the loop function $G^{\rho}{}_{D(D^*)(N,\Delta)}(P^0,\vec{P})$ as given in Eqs. (20) and (21).

III. RESULTS

We start this section by displaying in Fig. 1 the squared amplitude of the $D^*N \to D^*N$ transition for different partial waves as a function of the center-of-mass energy P^0 for a total momentum $|\vec{P}| = 0$. In particular, we show certain partial waves and energy regimes where we can find seven resonances predicted by the SU(8) model [57] that have or can have experimental confirmation [62], that is, $(I=0, J=1/2)$ $\Lambda_c(2595)$, $(I=1, J=1/2)$ $\Sigma_c(2823)$ and $\Sigma_c(2868)$, $(I=0,$

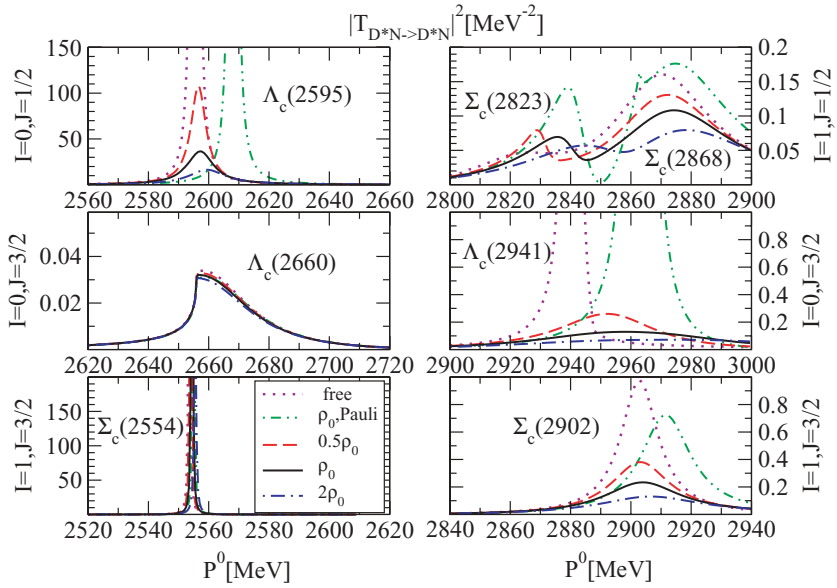

FIG. 1. (Color online) Square of the $D^*N \to D^*N$ amplitude for different partial waves as a function of the center-of-mass energy P^0 for fixed total momentum $|\vec{P}| = 0$. Several resonances are shown: $(I=0,\ J=1/2)$ $\Lambda_c(2595)$, $(I=1,\ J=1/2)$ $\Sigma_c(2823)$ and $\Sigma_c(2868)$, $(I=0,\ J=3/2)$ $\Lambda_c(2660)$, $(I=0,\ J=3/2)$ $\Lambda_c(2941)$, $(I=1,\ J=3/2)$ $\Sigma_c(2554)$, and $(I=1,\ J=3/2)$ $\Sigma_c(2902)$.

$J = 3/2$) $\Lambda_c(2660)$, ($I = 0$, $J = 3/2$) $\Lambda_c(2941)$, ($I = 1$, $J = 3/2$) $\Sigma_c(2554)$, and ($I = 1$, $J = 3/2$) $\Sigma_c(2902)$ resonances. All of them couple to the D^*N despite not being the dominant one for $\Lambda_c(2660)$, $\Sigma_c(2823)$, and $\Sigma_c(2554)$, as discussed in Ref. [57]. However, we choose to display these amplitudes for different nuclear densities, as they determine the D^* self-energy, as follows from Eq. (24). We analyze three cases in Fig. 1: (i) solution of the on-shell Bethe-Salpeter equation in free space (dotted lines), which was studied in Ref. [57]; (ii) in-medium calculation of the on-shell Bethe-Salpeter equation including Pauli blocking on the nucleon intermediate states at normal nuclear matter density $\rho_0 = 0.17\,\mathrm{fm}^{-3}$ (dashed lines); and (iii) the in-medium solution that incorporates Pauli blocking effects and D and D^* self-energies in a self-consistent manner for three densities, ranging from $0.5\rho_0$ to $2\rho_0$ (solid lines).

The $\Lambda_c(2595)$ resonance is predominantly a D^*N bound state, in contrast to the SU(4) TVME model, where it emerged as a DN quasibound state [18,36–38,48,49]. Pauli blocking effects on the intermediate nucleon states move the resonance to higher energies, as already found in previous in-medium models [35,38,48], due to the restriction of available phase space in the unitarization procedure. The shift in mass is of the order of 12 MeV, whereas for the SU(4) TVME model in Ref. [38] the shift is about a factor of 2 larger. This change in the energy shift provided by Pauli blocking can be attributed either to the different SU(4) and SU(8) kernels, or to the renormalization scheme employed to make the loop function finite, or to a combination of both effects. To distinguish among them, in Fig. 2 we examine the $\Lambda_c(2595)$ resonance in the $DN \to DN$ transition using the SU(4) TVME model

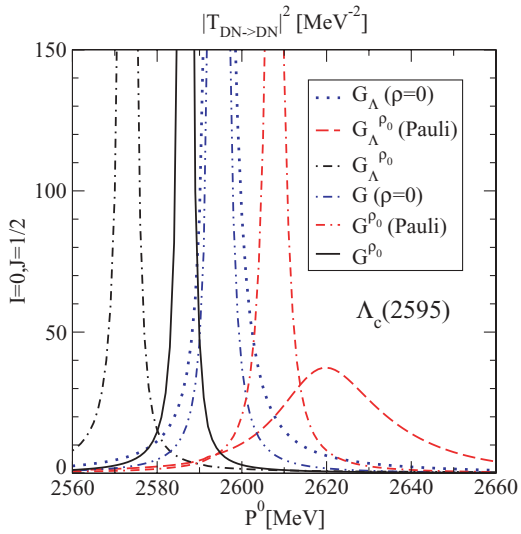

FIG. 2. (Color online) Square of the $DN \to DN$ amplitude in the ($I = 0$, $J = 1/2$) $\Lambda_c(2595)$ channel as a function of the center-of-mass energy P^0 with $|\vec{P}| = 0$. We show results with the SU(4) TVME model with a three-momentum cutoff ($\Lambda = 787$ MeV/c), as in Ref. [38], and, for comparison, we also show results using the renormalization scheme assumed in this work ($\alpha = 0.895$) [Eqs. (16) and (17)]. We examined three cases: free amplitude, calculation including Pauli blocking effects at $\rho = \rho_0$, and in-medium self-consistent solution at ρ_0.

(with $\Sigma_{DN} = 0$) in Ref. [38] for cases (i) to (iii). We compare results obtained using cutoff regularization [38] versus our new renormalization scheme [Eqs. (16) and (17)].[4] A similar mass shift for $\Lambda_c(2595)$ is observed in both the SU(4) and the SU(8) models when Pauli blocking effects are included for the new renormalization scheme. Therefore, we conclude that the different renormalization of the loop function is the main source of discrepancy; that is, the in-medium solution depends strongly on the correct treatment of the $\sqrt{s}$ dependence of the loop function. The treatment proposed here is clearly an improvement over those based on the use of a cutoff. Thus, the resonances that are far off-shell from their dominant channel will be heavily affected, as in the case of $\Lambda_c(2595)$. The self-consistent procedure moves the resonance closer to the free position because the repulsive effect of Pauli blocking is tamed by the inclusion of the D and D^* self-energies. In this case, the difference between the SU(8) and the SU(4) models is due not only to the renormalization scheme but also to the inclusion of the D^* self-energy, which compensates for the attraction felt by the D mesons, as we will see in the next figures.

The ($I = 1$, $J = 1/2$) $\Sigma_c(2823)$ and $\Sigma_c(2868)$ resonances are shown in the top-right panel in Fig. 1. Although no experimental evidence of these resonances is available yet, they lie very close to the DN threshold, and therefore, changes in the nuclear medium will have an important effect on the D self-energy, which is a matter of interest in this work. In fact, these resonant states are significantly modified in the medium, as both resonances couple significantly to DN and D^*N systems, as well as $D^*\Delta$, and any medium modification in those systems alters their behavior.

The next resonance predicted by the SU(8) model [57], ($I = 0$, $J = 3/2$) $\Lambda_c(2660)$, might be identified with the experimental $\Lambda_c(2625)$, which is the charm counterpart of $\Lambda(1520)$. This state couples strongly to the $\Sigma_c^*\pi$ channel and more weakly to the D^*N pair. Pauli blocking and self-consistency have smaller effects than in the case of the $\Lambda_c(2595)$ resonance. This is because, whereas the $\Lambda_c(2595)$ resonance varies in the medium due to the changes affecting its two dominant channels, D^*N and DN, the $\Lambda_c(2660)$ resonance is only modified via the secondary D^*N channel. We do not include any medium modifications affecting its dominant channel, $\pi\Sigma_c^*$. Although the pion self-energy [60,61] may induce some changes in this resonance, the expected effect of these modifications in the D and D^* self-energies is minor. On one hand, this partial wave will only have a direct contribution to the D^* self-energy, and thus the D self-energy will be affected indirectly via the simultaneous self-consistent calculation of the D and D^* self-energies. On the other hand, the effect of this resonance in the D^* self-energy is marginal because it is only reflected in the low-energy tail, far from the quasiparticle peak. Thus, we refrain from introducing any medium changes to this channel.

The ($I = 0$, $J = 3/2$) $\Lambda_c(2941)$ resonance might be a candidate for the experimental $\Lambda_c(2940)$, for which J^P is unknown [62]. This correspondence is made under the

[4] We now fix $\alpha = 0.895$ to obtain the correct position of $\Lambda_c(2595)$.

assumption that our model needs an additional implementation of p-wave interactions to explain the decay into $D^0 p$ pairs reported in Ref. [7], which is also suggested by the dominant coupling to D^*N. This strong coupling changes its properties significantly when medium modifications are implemented. Moreover, the fact that the $\Lambda_c(2941)$ resonance lies so close to the D^*N threshold will have important consequences for the D^* self-energy and, hence, for the spectral function, as we will see in the following.

The $(I = 1, J = 3/2)$ $\Sigma_c(2554)$ resonance has not yet been confirmed experimentally. However, similarly to $\Lambda_c(2660)$, this resonance might be the counterpart of the $\Sigma(1670)$ resonance in the charm sector. It couples strongly to $D\Delta$ and $D^*\Delta$ channels, which correspond to $\bar{K}\Delta$ in the strange sector. Pauli blocking effects on the nucleons are relatively weak because the coupling to the D^*N channel is approximately half the coupling to the two dominant channels. Changes due to the self-consistent procedure are comparable to the case for $\Lambda_c(2660)$.

The $\Sigma_c(2902)$ resonance in the $(I = 1, J = 3/2)$ sector could be a candidate for the $\Sigma_c(2800)$ resonance, with slight variation of the renormalization scale and if this resonance is also seen in $\pi\pi\Lambda_c$ states [57]. This is in contrast to the SU(4) TVME models, which predict it in the $I = 1$, $J = 1/2$, channel [36–38,48]. With regard to medium effects, they are comparable to those for the $\Lambda_c(2595)$ case. The dominant channel for the generation of this resonance is D^*N. Moreover, this resonance lies 50 MeV below the D^*N threshold. Therefore, modifications due to Pauli blocking and self-consistency are expected to be more important than for $\Lambda_c(2660)$ and $\Sigma_c(2554)$ and turn out to be comparable to the changes in $\Lambda_c(2595)$.

The left and right panels in Fig. 3 show the D and D^* self-energies, respectively, as functions of the meson energy q^0. The D and D^* self-energies result from the integration over the DN and D^*N amplitudes, respectively, after self-consistency

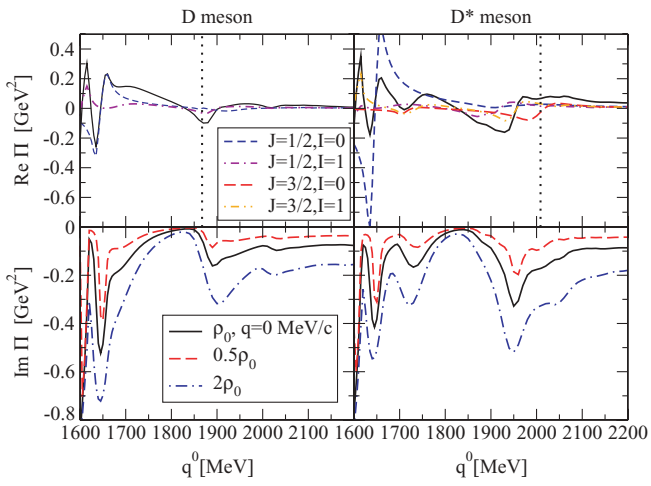

FIG. 3. (Color online) Real and imaginary parts of the D and D^* self-energies as functions of the meson energy q^0, including the decomposition in partial waves (upper panels), and for different densities at $q = 0$ MeV/c (lower panels). The positions of the D and D^* meson masses are also shown as dotted vertical lines for reference.

is reached simultaneously. The upper panels show the real part of the self-energies for ρ_0 at zero meson momentum (solid lines) together with the partial wave decomposition (dashed and dash-dotted lines). The partial waves weighted by the corresponding factors in Eqs. (23) and (24) are summed to obtain the total self-energies. The lower panels show the imaginary part of the self-energies for densities ranging from $0.5\rho_0$ to $2\rho_0$ and $q = 0$ MeV/c (solid lines). The dotted vertical lines in the upper panels indicate the free D and D^* meson masses.

With regard to the D meson self-energy, we observe that in the $I = 0$, $J = 1/2$ partial wave the contribution of the $\Lambda_c(2595)$ resonance clearly appears for energies of the D meson around 1650 MeV, whereas the resonant state $\Sigma_c(2556)$ governs the $I = 1$, $J = 1/2$ partial wave around $q^0 = 1615$ MeV. This state couples mostly to $D^*\Delta$, mixed with DN and $D_s^*\Sigma^*$, and it is absent in the SU(4) models [18,36–38,48], which do not include channels with a vector meson and a $3/2^+$ baryon. Close to the DN threshold ($\sqrt{s} = 2806$ MeV in free space), $I = 1$, $J = 1/2$ is the dominant partial wave. This is a consequence of the fact that this threshold lies very close to a resonant state in sector $I = 1$, $J = 1/2$ of 2823 MeV with a width of $\Gamma = 35$ MeV. This resonance is affected by Pauli blocking and self-consistency, that is, by the nuclear medium, as it couples strongly to states with D, D^*, and nucleon content. Closer to that structure, we also found a very narrow state in $I = 0$, $J = 1/2$, with a mass of 2821 MeV. This resonant state is less modified in the medium, as it couples marginally to the DN channel. Because of its narrow width even in nuclear matter, the main contribution to the D-meson self-energy close to the DN threshold comes from the $J = 1/2\Sigma_c(2823)$ resonance but modified by the near resonance $J = 1/2\Sigma_c(2868)$. These resonances lie above the DN threshold and, hence, have an attractive effect at the DN threshold.

The imaginary part of the D meson self-energy, in absolute value, grows with increasing density because of an enhancement of collision and absorption processes. The change in density can be seen more easily in the spectral function, as shown in Fig. 4. Compared to previous results in nuclear matter [35,38,47–49], the density dependence of the D meson self-energy is qualitatively similar. However, in the SU(8) model, we have a richer spectrum of resonant states that is reflected in the self-energy. Whereas $\Lambda_c(2595)N^{-1}$ and $\Sigma_c(2800)N^{-1}$ determine the D meson self-energy in SU(4) models [38,48], these contributions together with a few other resonant-hole states around $q^0 = 1860$–2060 MeV, such as $\Sigma_c(2823)N^{-1}$ and $\Sigma_c(2868)N^{-1}$, clearly manifest also in the D self-energy using the SU(8) interaction [57].

A novelty of the SU(8) model is that it allows one to simultaneously obtain the D and D^* self-energies. The D^* self-energy comes from the contribution not only from the $J = 1/2$ partial waves but also from the $J = 3/2$ waves of the D^*N amplitude. As expected in the $J = 1/2$ sector, we find the $\Lambda_c(2595)N^{-1}$ and $\Sigma_c(2556)N^{-1}$ components for $q^0 = 1650$ MeV and $q^0 = 1615$ MeV, respectively. For higher energies, around $q^0 = 1880$–1930 MeV, we see the $\Sigma_c(2823)N^{-1}$ and $\Sigma_c(2868)N^{-1}$ contributions. In the $J = 3/2$ sector, we find $\Sigma_c(2554)N^{-1}$ for $q^0 = 1610$ MeV. Close

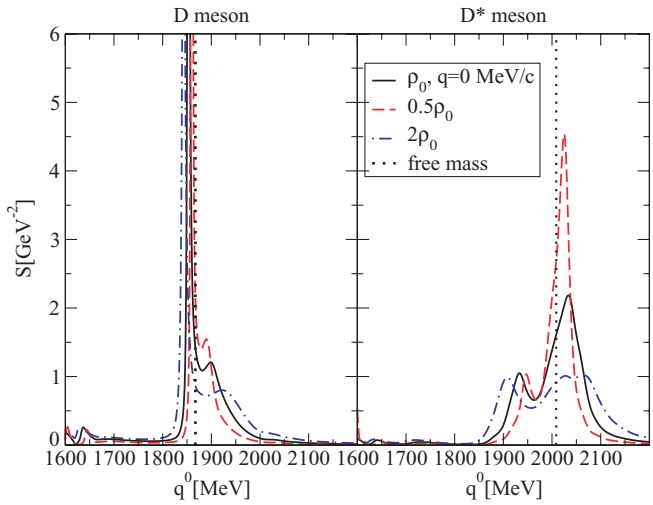

FIG. 4. (Color online) D and D^* spectral functions as a function of the meson energy q^0 for different densities at $q = 0$ MeV/c. The positions of the D and D^* meson free masses are also shown for reference (dotted vertical lines).

to the D^*N threshold ($\sqrt{s} = 2947$ MeV in free space), around $q^0 = 1960$ MeV, the $\Sigma_c(2902)N^{-1}$ excitation becomes dominant. This resonant-hole state mixes with $\Lambda_c(2941)N^{-1}$. The combination of both $J = 3/2$ resonances becomes the dominant contribution close to the D^*N threshold and has a repulsive effect on the D^* self-energy, as shown in the upper right panel in Fig. 4. Density effects have an outcome similar to that in the case of D self-energy. Those effects are better visualized with the spectral function.

The spectral functions for D and D^* mesons as a function of the meson energy q^0 are displayed in the left and right panels in Fig. 4, respectively. The solid lines correspond to the spectral functions at zero momentum from $0.5\rho_0$ to $2\rho_0$ for $|\vec{q}| = 0$ MeV/c. A dotted vertical line indicating the free D and D^* meson masses is also drawn for reference.

The quasiparticle peak of the spectral function, which is defined as

$$\omega_{\rm qp}(\vec{q})^2 = \vec{q}^2 + m^2 + {\rm Re}\Pi[\omega_{\rm qp}(\vec{q}), \vec{q}], \tag{25}$$

moves to lower energies with respect to the free mass position for the D meson as the density increases. As mentioned for Fig. 3, the presence of the $J = 1/2$ $\Sigma_c(2823)$ and $\Sigma_c(2868)$ resonances above the threshold has an attractive effect at the DN threshold. In fact, these resonances can be clearly seen on the right-hand side of the quasiparticle peak. In the low-energy tail of the D spectral function, for energies around 1600–1650 MeV, we observe the $\Sigma_c(2556)N^{-1}$ and $\Lambda_c(2595)N^{-1}$ excitations. Moreover, other wider resonances are generated in the SU(8) model [57] and they combine to give the total D meson spectral function. In the SU(4) TVME models [38,48,49], the $J = 1/2$ $\Sigma_c(2800)N^{-1}$ excitation fully mixes with the quasiparticle peak, whereas $\Lambda_c(2595)N^{-1}$ appears at the same energies as in our SU(8) model, as expected.

The quasiparticle peak of the D^* spectral function moves to higher energies with density and fully mixes with the subthreshold $J = 3/2\Lambda_c(2941)$ resonance. In the left-hand side of the peak we observe the mixing of the $J = 1/2$ $\Sigma_c(2868)N^{-1}$ and $J = 3/2\Sigma_c(2902)N^{-1}$ excitations. Other dynamically generated particle-hole states appear for higher and lower energies, such as $J = 3/2\Sigma_c(2554)N^{-1}$.

Density effects result in a broadening of the spectral functions as the collisional and absorption processes increase together with a dilution of the resonant-hole states. This outcome is qualitatively similar to previous models for the D meson spectral function [35,38,47–49].

As already mentioned in Ref. [49], the low-energy tail of the D meson spectral function due to resonant-hole states ($\tilde{Y}_c N^{-1}$) might shed light on the J/Ψ suppression in a hadronic scenario. However, it is unlikely that this lower tail extends with sufficient strength as far as the J/Ψ threshold to explain J/Ψ suppression only via the $D\bar{D}$ decay. A more plausible hadronic contribution for the J/Ψ suppression is the reduction of its supply from the excited charmonia, $\chi_{c\ell}(1P)$ or Ψ', which may find other competitive decay channels in the medium [49]. Such a broader scenario for J/Ψ suppression has been suggested recently in thermal models [63]. On the other hand, the spectral function for the D and D^* mesons will influence the behavior of dynamically generated hidden and open charm scalar resonances in nuclear matter, as pointed out in Ref. [64].

Finally, we study the properties of D and D^* mesons close to the DN and D^*N threshold. We first present, in Table II, results for the DN and D^*N effective interactions in free space. In particular, we give the $J = 1/2$ and $J = 3/2$ scattering lengths for $I = 0$ and $I = 1$,

$$a^{IJ}_{D(D^*)N} = -\frac{1}{4\pi}\frac{M_N}{\sqrt{s}} T^{IJ}_{D(D^*)N\to D(D^*)N}, \tag{26}$$

at $D(D^*)N$ threshold and with M_N the nucleon mass. For the DN effective interaction, we find that our $I = 0$ scattering length is negligible compared to the $I = 1$ one, in contrast to the SU(4) TVME model in Ref. [48] or the meson-exchange model of the Jülich group [40]. Moreover, our positive scattering lengths indicate the attractive behavior of the D meson self-energy close to threshold, in contrast with the values in those previous references. The discrepancy with previous works has its origin in the different resonant-hole composition of the self-energy close to threshold. Moreover, as a new development, we also provide the D^*N scattering lengths. We note that the dominant repulsive contribution comes from the $J = 3/2$ partial wave.

TABLE II. DN and D^*N scattering lengths (in fm).

	DN	D^*N
$J = 1/2$, $I = 0$	0.001 + i 0.002	$-0.44 + i0.19$
(Born approx.)	(0.59 + i 0)	$(1.82 + i0)$
$J = 1/2$, $I = 1$	0.33 + i 0.05	$-0.36 + i0.18$
(Born approx.)	(0.20 + i 0)	$(0.07 + i0)$
$J = 3/2$, $I = 0$		$-1.93 + i0.19$
(Born approx.)		(0 + i 0)
$J = 3/2$, $I = 1$		$-0.57 + i0.15$
(Born approx.)		$(0.27 + i0)$

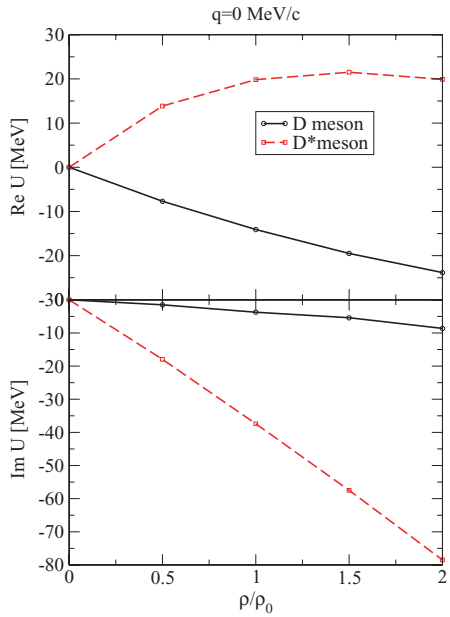

FIG. 5. (Color online) D and D^* optical potentials as a function of ρ/ρ_0 for $|\vec{q}| = 0$ MeV/c.

Calculated scattering lengths come out radically different from those deduced within the Born approximation. This is not surprising because of the strong character of the meson-baryon interaction in the $C = 1$ sector and the existence of resonances that hint at nonperturbative physics close to the $D^{(*)}N$ threshold (and in some cases they are even placed below it).

We can now define the D and D^* optical potentials in the nuclear medium as

$$U(\vec{q}) = \frac{\Pi[\omega_{qp}(\vec{q}), \vec{q}]}{2\sqrt{m^2 + \vec{q}^2}}, \tag{27}$$

which, at zero momentum, can be identified as the in-medium shift of the D and D^* meson mass. In Fig. 5 the real and imaginary parts of the optical potential are shown as a function of the density for $|\vec{q}| = 0$ MeV/c. The symbols indicate the values calculated for the optical potentials. We refrain from showing finite-momentum results for the optical potential because of the uncertainties present in our calculation once we move away from the threshold, as a result of the WT interaction together with the ignoring of higher multipolarity interactions.

The mass shift at $\rho = \rho_0$ stays attractive for the D meson, whereas it becomes repulsive for the D^* meson with increasing density, in correspondence with the behavior of the quasiparticle peaks in Fig. 4. Similar values for the D meson potential were obtained for in-medium models in Refs. [35,38,47–49]. However, as explained for Fig. 4, the origin of the attraction can be traced back to a different resonant-hole contribution in the SU(4) models compared to the SU(8) case.

The dilution of the spectral functions with density gives rise to the increase in the imaginary part of the optical potential for both D and D^* mesons, as this corresponds in the model to half the width of the spectral function at the quasiparticle peak. However, the D meson width turns out to be much smaller in the SU(8) scheme than in the SU(4) models. Thus, we expect to find bound states for the D^0-nucleus system [41]. Looking at the strength of the optical potential for density ρ_0, we expect those states to be bound by at most 15 MeV and to have half-widths lower than 4 MeV. Hence, we expect various states to be observable in different nuclei. It would be of interest to study the D^0-nucleus spectrum, binding energies, and widths predicted by the optical potential obtained here and compare them with predictions of other models. It is not clear whether the D^+-nucleus hadronic attraction will be able to overcome the Coulomb repulsion to provide similar bound states; this will be a subject of future research. Experiments to determine such D^0-nucleus bound states would be welcome.

IV. CONCLUSIONS

We have studied the properties of D and D^* mesons in symmetric nuclear matter within a simultaneous self-consistent coupled-channel unitary approach that implements the features of HQS. The corresponding in-medium solution incorporates Pauli blocking effects and D and D^* meson self-energies in a self-consistent manner. In particular, we have analyzed the behavior of dynamically generated baryonic resonances in the nuclear medium in the $C = 1$ and $S = 0$ sector within this SU(8) spin-flavor symmetric model and their influence on the self-energy and, hence, the spectral function of D and D^* mesons. We have also obtained the D and D^* scattering lengths and computed optical potentials for different density regimes. We have, finally, compared our results with those of previous SU(4) models [38,40,48,49], paying special attention to the renormalization of the intermediate propagators in the medium beyond the usual cutoff scheme.

The SU(8) model generates a wider spectrum of resonances with $C = 1$ and $S = 0$ content compared to the previous SU(4) models. Whereas the parameters of both SU(4) and SU(8) models are fixed by the $(I = 0, J = 1/2)$ $\Lambda_c(2595)$ resonance, the incorporation of vector mesons in the SU(8) scheme generates naturally $J = 3/2$ resonances, such as $\Lambda_c(2660)$, $\Lambda_c(2941)$, $\Sigma_c(2554)$, and $\Sigma_c(2902)$, which might be identified experimentally [62]. New resonances are also produced for $J = 1/2$, such as $\Sigma_c(2823)$ and $\Sigma_c(2868)$, whereas others are not observed due to the different symmetry breaking pattern used in both models. The modifications of the mass and width of these resonances in the nuclear medium will strongly depend on the coupling to channels with D, D^*, and nucleon content. Moreover, resonances close to the DN or D^*N thresholds change their properties more evidently compared to those far off-shell. The improvement of the regularization and renormalization procedure for the intermediate propagators in the nuclear medium beyond the usual cutoff method also has an important effect on the in-medium changes of the dynamically generated resonances, in particular, for those lying far off-shell from their dominant channel, as in the case of $\Lambda_c(2595)$.

The self-energy and, hence, the spectral function of D and D^* mesons thus show a rich spectrum of resonant-hole states. The D meson quasiparticle peak mixes strongly with $\Sigma_c(2823)N^{-1}$ and $\Sigma_c(2868)N^{-1}$ states, whereas

$\Lambda_c(2595)N^{-1}$ is clearly visible in the low-energy tail. The D^* spectral function incorporates the $J = 3/2$ resonances, and the $\Sigma_c(2902)N^{-1}$ and $\Lambda_c(2941)N^{-1}$ fully mix with the quasiparticle peak. As the density increases, these $\tilde{Y}_c N^{-1}$ modes tend to smear out and the spectral functions broaden as the collisional and absorption processes increase. This broadening in dense matter might have important consequences for the dynamic generation of scalar resonances with hidden and open charm content [64] as well as for excited charmonium states for the experimental conditions expected in the PANDA and CBM experiments at FAIR [2]. The latter experimental scenario, however, requires the incorporation of finite-temperature effects.

The behavior with density of the quasiparticle peaks is better visualized with the optical potentials. The D meson potential stays attractive, whereas the D^* meson one is repulsive with increasing density up to twice the normal nuclear matter one. The attractive and repulsive character of the DN and D^*N interactions close to threshold, respectively, was already observed in free space via the scattering lengths. In particular, the optical potentials with density do not follow the low-density approximation, as expected from the complicated resonant-hole structure of the self-energy. The imaginary part in both cases increases with the density. Compared to in-medium SU(4) TVME models, we obtain similar values for the D meson real part of the potential but much smaller imaginary parts. This result could have important implications for the observation of D^0-nucleus bound states. Work along this line is in progress.

Future work will also include study of the influence of the Δ self-energy on the in-medium D and D^* self-energies as well as the inclusion of the width of the vector mesons in the meson-baryon channels. Moreover, finite-temperature effects are mandatory for analysis and interpretation of the data from the future CBM heavy-ion experiment at FAIR.

To close, we would like to stress that it will be important to count with an improved model in vacuum, and future research along these lines would be highly desirable. Considering the findings of this work, one should bear in mind that the deficiencies of the model in free space will definitely affect the results presented here for amplitudes embedded in cold nuclear matter.

ACKNOWLEDGMENTS

C.G.R. thanks L. L. Salcedo for useful discussions. L.T. wishes to acknowledge support from the RFF-Open and Hidden Charm at the PANDA project of the Rosalind Franklin Programme at the University of Groningen (The Netherlands) and the Helmholtz International Center for FAIR within the framework of the LOEWE program of the State of Hesse (Germany). This research was supported by DGI and FEDER funds, under Contract No. FIS2008-01143/FIS and the Spanish Consolider-Ingenio 2010 Programme CPAN (CSD2007-00042), and by Junta de Andalucía under Contract No. FQM225. It is part of the European Community-Research Infrastructure Integrating Activity "Study of Strongly Interacting Matter" (acronym HadronPhysics2; Grant Agreement No. 227431) and of the European Union Human Resources and Mobility Activity LAVIAnet (Contract No. MRTN-CT-2006-035482), under the Seventh Framework Programme of the European Union.

[1] T. Matsui and H. Satz, Phys. Lett. **B178**, 416 (1986).
[2] http://www.gsi.de/fair/.
[3] M. Artuso *et al.* (CLEO Collaboration), Phys. Rev. Lett. **86**, 4479 (2001).
[4] R. Mizuk *et al.* (Belle Collaboration), Phys. Rev. Lett. **94**, 122002 (2005).
[5] R. Chistov *et al.* (BELLE Collaboration), Phys. Rev. Lett. **97**, 162001 (2006).
[6] B. Aubert *et al.* (BABAR Collaboration), Phys. Rev. Lett. **97**, 232001 (2006).
[7] B. Aubert *et al.* (BABAR Collaboration), Phys. Rev. Lett. **98**, 012001 (2007).
[8] R. Mizuk *et al.* (Belle Collaboration), Phys. Rev. Lett. **98**, 262001 (2007).
[9] N. Kaiser, P. B. Siegel, and W. Weise, Nucl. Phys. **A594**, 325 (1995).
[10] N. Kaiser, P. B. Siegel, and W. Weise, Phys. Lett. **B362**, 23 (1995).
[11] E. Oset and A. Ramos, Nucl. Phys. **A635**, 99 (1998).
[12] B. Krippa, Phys. Rev. C **58**, 1333 (1998); B. Krippa and J. T. Londergan, *ibid.* **58**, 1634 (1998).
[13] J. C. Nacher, A. Parreno, E. Oset, A. Ramos, A. Hosaka, and M. Oka, Nucl. Phys. **A678**, 187 (2000).
[14] U. G. Meissner and J. A. Oller, Nucl. Phys. **A673**, 311 (2000).
[15] J. A. Oller and U. G. Meissner, Phys. Lett. **B500**, 263 (2001).
[16] J. Nieves and E. Ruiz Arriola, Phys. Rev. D **64**, 116008 (2001).
[17] T. Inoue, E. Oset, and M. J. Vicente Vacas, Phys. Rev. C **65**, 035204 (2002).
[18] M. F. M. Lutz and E. E. Kolomeitsev, Nucl. Phys. **A700**, 193 (2002).
[19] C. García-Recio, J. Nieves, E. Ruiz Arriola, and M. J. Vicente Vacas, Phys. Rev. D **67**, 076009 (2003).
[20] E. Oset, A. Ramos, and C. Bennhold, Phys. Lett. **B527**, 99 (2002).
[21] A. Ramos, E. Oset, and C. Bennhold, Phys. Rev. Lett. **89**, 252001 (2002).
[22] D. Jido, J. A. Oller, E. Oset, A. Ramos, and U. G. Meissner, Nucl. Phys. **A725**, 181 (2003).
[23] L. Tolós, A. Ramos, A. Polls, and T. T. S. Kuo, Nucl. Phys. **A690**, 547 (2001).
[24] C. García-Recio, M. F. M. Lutz, and J. Nieves, Phys. Lett. **B582**, 49 (2004).
[25] J. A. Oller, J. Prades, and M. Verbeni, Phys. Rev. Lett. **95**, 172502 (2005).
[26] B. Borasoy, R. Nissler, and W. Weise, Eur. Phys. J. A **25**, 79 (2005).
[27] B. Borasoy, U. G. Meissner, and R. Nissler, Phys. Rev. C **74**, 055201 (2006).
[28] T. Hyodo, D. Jido, and A. Hosaka, Phys. Rev. C **78**, 025203 (2008).
[29] A. Ramos and E. Oset, Nucl. Phys. **A671**, 481 (2000).

[30] L. Tolós, A. Ramos, and A. Polls, Phys. Rev. C **65**, 054907 (2002).
[31] L. Tolós, D. Cabrera, A. Ramos, and A. Polls, Phys. Lett. **B632**, 219 (2006).
[32] L. Tolós, A. Ramos, and E. Oset, Phys. Rev. C **74**, 015203 (2006).
[33] L. Tolós, D. Cabrera, and A. Ramos, Phys. Rev. C **78**, 045205 (2008).
[34] D. Cabrera, A. Polls, A. Ramos, and L. Tolós, Phys. Rev. C **80**, 045201 (2009).
[35] L. Tolós, J. Schaffner-Bielich, and A. Mishra, Phys. Rev. C **70**, 025203 (2004).
[36] J. Hofmann and M. F. M. Lutz, Nucl. Phys. **A763**, 90 (2005).
[37] J. Hofmann and M. F. M. Lutz, Nucl. Phys. **A776**, 17 (2006).
[38] T. Mizutani and A. Ramos, Phys. Rev. C **74**, 065201 (2006).
[39] J. Haidenbauer, G. Krein, U. G. Meissner, and A. Sibirtsev, Eur. Phys. J. A **33**, 107 (2007).
[40] J. Haidenbauer, G. Krein, U. G. Meissner, and A. Sibirtsev, Eur. Phys. J. A **37**, 55 (2008).
[41] K. Tsushima, D. H. Lu, A. W. Thomas, K. Saito, and R. H. Landau, Phys. Rev. C **59**, 2824 (1999).
[42] A. Sibirtsev, K. Tsushima, and A. W. Thomas, Eur. Phys. J. A **6**, 351 (1999).
[43] A. Hayashigaki, Phys. Lett. **B487**, 96 (2000).
[44] A. Mishra, E. L. Bratkovskaya, J. Schaffner-Bielich, S. Schramm, and H. Stöcker, Phys. Rev. C **70**, 044904 (2004).
[45] T. Hilger, R. Thomas, and B. Kampfer, Phys. Rev. C **79**, 025202 (2009).
[46] A. Mishra and A. Mazumdar, Phys. Rev. C **79**, 024908 (2009).
[47] L. Tolós, J. Schaffner-Bielich, and H. Stoecker, Phys. Lett. **B635**, 85 (2006).
[48] M. F. M. Lutz and C. L. Korpa, Phys. Lett. **B633**, 43 (2006).
[49] L. Tolós, A. Ramos, and T. Mizutani, Phys. Rev. C **77**, 015207 (2008).
[50] S. Sarkar, B. X. Sun, E. Oset, and M. J. V. Vacas, arXiv:0902.3150 [hep-ph].
[51] E. Oset, P. Gonzalez, M. J. V. Vacas, A. Ramos, J. Vijande, S. Sarkar, and B. X. Sun, presented at the International Workshop on Effective Field Theories: From the Pion to the Upsilon, Valencia, February 2009, arXiv:0904.4804 [nucl-th].
[52] E. Oset and A. Ramos, arXiv:0905.0973 [hep-ph].
[53] C. García-Recio, J. Nieves, and L. L. Salcedo, Phys. Rev. D **74**, 034025 (2006).
[54] C. García-Recio, J. Nieves, and L. L. Salcedo, Phys. Rev. D **74**, 036004 (2006).
[55] C. García-Recio, J. Nieves, and L. L. Salcedo, Eur. Phys. J. A **31**, 499 (2007); **31**, 540 (2007).
[56] H. Toki, C. García-Recio, and J. Nieves, Phys. Rev. D **77**, 034001 (2008).
[57] C. García-Recio, V. K. Magas, T. Mizutani, J. Nieves, A. Ramos, L. L. Salcedo, and L. Tolós, Phys. Rev. D **79**, 054004 (2009).
[58] J. Nieves and E. Ruiz Arriola, Phys. Lett. **B455**, 30 (1999).
[59] J. Nieves and E. Ruiz Arriola, Nucl. Phys. **A679**, 57 (2000).
[60] J. Nieves, E. Oset, and C. García-Recio, Nucl. Phys. **A554**, 509 (1993).
[61] J. Nieves, E. Oset, and C. García-Recio, Nucl. Phys. **A554**, 554 (1993).
[62] W.-M. Yao *et al.*, J. Phys. G **33**, 1 (2006).
[63] A. Andronic, P. Braun-Munzinger, K. Redlich, and J. Stachel, Phys. Lett. **B659**, 149 (2008).
[64] R. Molina, D. Gamermann, E. Oset, and L. Tolós, Eur. Phys. J. A **42**, 31 (2009).